

Studies of the aurorally-induced ultraviolet
emissions on the nightside of Venus

Report for period 1/1/85-3/31/86

Pioneer Venus Guest Investigator

Grant NAG2-329

J. L. Fox

Laboratory for Planetary Atmospheres Research
and Department of Mechanical Engineering

SUNY-Stony Brook

Stony Brook, New York

(NASA-CR-177004) STUDIES OF THE
AURORALLY-INDUCED ULTRAVIOLET EMISSIONS ON
THE NIGHTSIDE OF VENUS Report, 1 Jan. 1985
- 31 Mar. 1986 (State Univ. of New York)
23 p

N86-31478

Unclas

CSSL 03B G3/91 43017

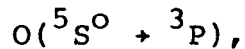
The Pioneer Venus Ultraviolet Spectrometer has detected emissions of atomic oxygen on the nightside of Venus which are too intense to be due to radiative recombination of O^+ .



and hence cannot be interpreted as nightglow, as they are on Earth (Julienne et al. 1974). The emissions at 1304 and 1356Å arise from the transitions



and



respectively. The measured intensities average about 20R for the 1304Å feature, although excursions to 100R have been observed; the ratio of the 1304Å intensity to the 1356Å intensity is about 5. We have been investigating the possibility that these emissions are caused by the precipitation of particles into the nightside atmosphere. We have first considered the effect of a flux of energetic electrons, both by analogy with the terrestrial aurora and because the cross sections for the interaction of energetic electrons with atmospheric species are fairly well known compared to the cross sections for proton or heavy particle impact.

The $^3S^0$ and $^5S^0$ excited states of atomic oxygen may be produced in the Venusian thermosphere by electron impact on CO_2 , CO and O:



and



Cross sections for (1) and (3) have been measured by Sroka (1970), Ajello (1971a), Mumma et al. (1972), and Ajello (1971b). Emission cross sections for electron impact excitation of atomic oxygen (2) have been reported by Stone and Zipf (1974) and recently modified by Zipf and Erdman (1985). The emission cross sections are comprised of the cross sections for direct excitation of the $^3S^0$ and $^5S^0$ states and the contribution due to cascading from higher excited states. The major cascade contribution to the 1304Å emission under optically thin conditions is due to excitation of the $^3P^e$ state, which decays into the $^3S^0$ state with the emission of an 8446Å photon; the main cascade contribution to the 1356Å emission is from the $^5P^e$ state, which decays into the $^5S^0$ state with the emission of a 7774Å photon. Several theoretical excitation cross sections are available for the $^3S^0$ and $^5S^0$ states and the states which cascade into them (e.g., Rountree and Henry, 1972; Rountree,

1979; Jackman et al., 1977). An experimental cross section for excitation of $^3S^0$ state at 100 eV has been reported recently by Doering et al. (1986).

The altitude at which electrons deposit their energy is determined by their energy: more energetic electrons penetrate to lower altitudes. Because the composition of the thermosphere changes with altitude, and because the excitation cross sections have different shapes as a function of energy, the spectrum of the electrons will determine the relative importance of processes 1-3, the ratios and intensities of the emissions, and therefore the number flux of electrons necessary to produce the observed emissions.

In addition to the observed intensities of 1304 and 1356 Å emission, other data are available which can be used to constrain the electron spectrum or to determine whether electron precipitation is a viable source for the emissions. First, no CO ($a^3\Pi \rightarrow X^1\Sigma^+$) Cameron band emission was detected on the nightside by the PVOUVS. An maximum of about 100R could be hidden beneath the NO nightglow. No O 5577 Å green line emission was detected by the visible spectrometers on the Venera 9 and 10 spacecraft. An upper limit of 10R has been placed on its intensity (Krasnopol'sky 1981 and private communication, 1985). In addition, values for the integral suprathermal electron flux in the Venus umbra between 1000 and 2000 km were measured by the Pioneer Venus Retarding

Potential Analyzer and reported by Knudsen and Miller (1985).

METHOD

We have examined the effect of a monoenergetic flux of electrons on a model atmosphere of the nightside thermosphere of Venus. The neutral model chosen is that of Hedin (1983) for high solar activity ($F_{10.7} = 200$) and 165° solar zenith angle. This model is based on measurements made by the Pioneer Venus Orbiter Neutral Mass Spectrometer (e.g., Niemann et al. 1980). We have included four species in the calculation: CO_2 , O, CO, and N_2 . The model atmosphere is shown in Figure 1.

The numerical method we have chosen for energy deposition of the primary electrons is the continuous slowing down approximation. In this approximation the energy of the electron E is given by

$$E = E_0 - \int_{\infty}^x \frac{dE}{dx} dx'$$

where E_0 is the initial energy and dE/dx is the stopping power:

$$\frac{dE}{dx} = \sum_i n_i L_i(E).$$

Here, n_i is the number density of species i and L is the loss function or stopping cross section:

$$L_i(E) = \sum_j \sigma_j(E)W_j + \int_0^{(E_p - I)/2} (I+W) \frac{d\sigma}{dW}(E_p, W) dW$$

where the σ_j are cross sections for excitation processes j , W_j are the corresponding excitation energies, $d\sigma/dW$ is the differential cross section for ionization by a primary electron of energy E_p to produce a secondary electron of energy W , and I is the ionization potential. The loss function for CO_2 has been calculated by Fox and Dalgarno (1979). Dalgarno and Lejeune (1971) have reported a loss function for atomic oxygen, although some of their cross sections are out of date. We have updated our CO_2 cross sections and our atomic oxygen cross sections to include those measured and calculated since these compilations and we have extended them to higher energies using the Bethe-Born form:

$$\frac{C_1}{E} \ln C_2 E$$

for allowed transitions and

$$\frac{C}{E}$$

for forbidden transitions. Because the scale height of the Venus atmosphere is small (about 3 km), the primary energy deposition calculation required the use of fine altitude grid with a resolution of 100m.

The secondary electron distribution was computed using the empirically determined shape of the differential cross section determined by Opal et al. (1971):

$$\frac{d\sigma}{dW}(E_p, W) = \frac{A(E_p)}{1 + \left(\frac{W}{\bar{W}}\right)^{2.1}}$$

where W is the energy of the secondary electron, \bar{W} is an empirically determined constant, and $A(E_p)$ is chosen so that the differential cross section is normalized to the measured value of the total ionization cross section. The secondary electrons are assumed to deposit their energy locally and discretely as discussed by Victor et al. (1976). This is a good approximation in the altitude range of maximum energy deposition since most of the secondary electrons have energies below 200 eV.

RESULTS

Calculations were performed for primary electrons with energies of 200, 300, 500, 600, 800 and 1000 eV. The distribution of angles of incidence was assumed to be isotropic from 0 to 75°. The computed altitude profiles of primary electron energy for initial energies of 200, 500 and 1000 eV are shown in Figure 2. The electrons at a given incident angle deposit their energy over a very small altitude range because the scale height of the atmosphere is

small. Much of the observed spread in the altitude of deposition is due to the assumption of isotropy of the electron flux.

The altitude at which the energy of the electron drops below 50 eV is 136, 131 and 128 km for 200, 500 and 1000 eV electrons, respectively. As we would expect, the higher energy primaries deposit their energy lower in the atmosphere. Since the altitude above which the primary constituent changes from CO₂ to O is about 140 km, the higher energy primaries deposit their energy mainly at an altitude at which the CO₂ density exceeds the atomic oxygen density. This fact will be reflected in the relative intensities of the emissions produced.

Since the ($O^5S^0 + ^3P$) transition is forbidden, radiative transfer is not as important in determining the intensity of the 1356Å emission as it is for the 1304Å resonance line. Thus we have chosen to normalize our calculations to the electron flux necessary to produce 4R of 1356Å emission. The flux obtained depends on the cross sections adopted. If we adopt the emission cross section of Stone and Zipf (1974) as modified by Zipf and Erdman (1985) the necessary energy flux varies from $1.6 \times 10^{10} \text{ eV cm}^{-2} \text{ s}^{-1}$ to $2.9 \times 10^{10} \text{ eV cm}^{-2} \text{ s}^{-1}$ for electron energies from 200 eV to 1 keV. If we adopt the excitation cross section of Rountree (1977) for the $O(^5S^0)$ state and add the cross section for

the $5p^e$ state suggested by Jackman et al. (1977), the necessary energy fluxes range from 1.2×10^{10} to 2.2×10^{10} eV $\text{cm}^{-2} \text{s}^{-1}$. The necessary number flux as a function of energy of the primary electron is shown in Figure 3, for both the Stone and Zipf cross section and the theoretical cross sections. The number flux is compared to one-half the upper limit on the omnidirectional flux reported by Knudsen and Miller (1985) from PV RPA measurements in the Venus umbra. Fewer electrons are necessary if the theoretical cross sections are adopted. The excitation and emission cross sections differ mostly in their low energy shapes. Since the major production of $O(5S)$, for soft electrons, is by secondary electron impact on O, the low energy shape is as important as the magnitude of the cross section at higher energies. The sensitivity of the results to the model atmosphere adopted was probed by doubling the atomic oxygen densities in the Hedin model. The necessary number flux for that case is also shown in Figure 3. If only the upper limit on the number flux is considered, it appears that energetic electrons are more likely than soft electrons as the source of the emissions.

In computing the production rate of $3S^o$ from the normalized electron fluxes, we also have a choice of cross sections. The emission cross sections reported by Stone and Zipf (1974) and Zipf and Erdman (1985) are appropriate to

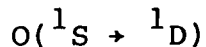
optically thin conditions only. The value of the cross section at 100 eV is about $11 \times 10^{-18} \text{ cm}^2$. Doering and Vaughan (1986) have reported a value of $6.4 \times 10^{-18} \text{ cm}^2$ for the excitation cross section at 100 eV from electron energy loss spectra. This value is in good agreement with the calculations of Rountree and Henry (1972). Although they report that the difference between the excitation and emission cross sections can be attributed to cascading, the bulk of the cascade contribution under optically thin conditions should come from states for which the transition to the ground state is forbidden. These states should not have significant cross sections at 100 eV. We conclude that the cross sections for excitation of the $3S^0$ state are also uncertain by up to a factor of two.

The 1304A emission is due to an allowed transition and a calculation of the intensity should involve a consideration of radiative transfer. In addition, under optically thick conditions, the cascade contribution will be enhanced, as has been shown by Julienne and Davis (1976). We calculate here only the production rates. The results are presented in Table 1 for the three normalizations of the electron flux. These values are computed using the 1304A emission cross sections of Zipf and Erdman (1985). The production rates appear to be sufficient for the softer electrons, although detailed radiative transfer calculations

must be done in order to predict the intensity. It would perhaps be better to normalize the electron flux to that necessary to produce 20R of 1304A emission; in the coming year we hope to do so.

Intensities of the contaminating emissions may also be calculated. The CO Cameron bands arise from the decay of the $a^3\Pi$ state and may be produced by electron impact on CO_2 or CO. The excitation function for production of CO ($a^3\Pi$) by dissociative electron impact on CO_2 has been measured by several workers, but the absolute magnitude of the cross section is uncertain. Estimates of the maximum cross section range from $3(-17)$ to $3(-16)$ cm^2 (Ajello, 1971a; Freund, 1971; Wells et al., 1972; Erdman and Zipf, 1983)). We have adopted the normalization required by Conway (1981) to reproduce the Mariner 9 dayglow measurements. Table 2 shows the computed intensities for the three normalizations of the electron flux. The upper limit set by the PVOUVS non-detection is exceeded for the more energetic electrons.

The atomic oxygen green line arises from the transition



The $\text{O}(^1\text{S})$ state may be produced by electron impact on CO_2 , CO, or O. A cross section for electron impact dissociative excitation of CO_2 has been constructed by Jackman et al.

(1977). Shyn et al. (1985) have recently reported a measurement of the cross section for direct excitation of atomic oxygen that is twice the theoretical value of Henry et al. (1969) that we have used in the past and that has been adopted by other workers. Table 3 shows our predicted intensities of 5577Å emission. Compared to the upper limit of 10 R placed on the intensity by the Venera measurements, our predicted intensities are rather large. The computed values, however, may be in error due to several effects. First, the cross section for direct electron impact excitation of atomic oxygen is sensitive to the fractional ionization. The electron density profiles that we have adopted correspond to average conditions; if the atmosphere were bombarded with significant flux of electrons, the electron densities might exceed the assumed densities. Table 4 illustrates the effect of fractional ionization on the $O(^1S)$ excitation rates. The table gives the energy lost in producing various excited states of atomic oxygen for a 100 eV primary electron depositing its energy in pure atomic oxygen. For fractional ionization of 2×10^{-4} , 0.65 eV are consumed in producing $O(^1S)$. If the fraction is reduced to 2×10^{-5} or less, 1 eV or more is used. Thus the production rate of $O(^1S)$ will be greatly reduced for higher fractional ionizations. Second, the steady state flux at low energies is sensitive to the assumed cross sections for vibrational

excitation of CO_2 , which have only been included in an approximate way in our compilations. Third, processes with small energy losses cannot be treated accurately with a 1 eV electron grid. We hope to remedy these problems in the coming year. It should be noted that only direct excitation of atomic oxygen is affected by these considerations; the threshold for dissociative excitation of CO_2 is 9.62 eV and the maximum cross section occurs near 70 eV. The cross section for this process however is not well known. Its value is based on generalized oscillator strength data, so the low energy shape should not be taken literally.

References

- Ajello, J. M., Emission cross sections of CO₂ by electron impact in the interval 1260-4500Å II, J. Chem. Phys. 55, 3169-3177, 1971a.
- Ajello, J. M., Emission cross sections of CO₂ by electron impact in the interval 1260-5000Å I, J. Chem. Phys. 55, 3158-3168., 1971b.
- Conway, R. R., Spectroscopy of the Cameron bands in the Mars airglow, J. Geophys. Res. 86, 4767-4775, 1981.
- Dalgarno, A. and G. Lejeune, The absorption of electrons in atomic oxygen, Planet. Space Sci. 19, 1653-1667, 1971.
- Doering, J. P., E. E. Gulcicek and S. O. Vaughan, Electron impact measurement of oscillator strengths for dipole-allowed transitions of atomic oxygen, J. Geophys. Res. 90, 5279-5284, 1983.
- Doering, J. P. and S. O. Vaughan, Absolute experimental differential and integral electron excitation cross sections for atomic oxygen. 1. The (³P → ³S⁰) transition (1304Å) at 100 eV, J. Geophys. Res. 91, 3279-3286, 1986.
- Erdman, P. W. and E. C. Zipf, Electron-impact excitation of the Cameron system (^a3Π → X¹Σ) of CO, Planet. Space Sci. 31, 317-321, 1983.
- Fox, J. L. and A. Dalgarno, Electron energy deposition in carbon dioxide, Planet. Space Sci. 27, 491, 1979.

- Freund, R. S., Dissociation of CO_2 by electron impact with the formation of metastable CO ($a^3\pi$) and O(5S), J. Chem. Phys. 55, 3569-3577, 1971.
- Hedin, A. E., H. B. Niemann, W. T. Kasprzak and A. Seiff, Global empirical model of the Venus thermosphere, J. Geophys. Res. 88, 73-83, 1983.
- Henry, R. J. W., P. G. Burke and A. L. Sinfailam, Phys. Rev. 178, 218, 1969.
- Jackman, C. H., R. H. Garvey and A. E. S. Green, Electron impact on atmospheric gases I. Updated cross sections, J. Geophys. Res. 82, 5081-5090, 1977.
- Julienne, P. S. and J. Davis, Cascade and radiation trapping effects on atmospheric atomic oxygen emission excited by electron impact, J. Geophys. Res. 81, 1397-1403, 1976.
- Julienne, P. S., J. Davis and E. Oran, Oxygen recombination in the tropical nightglow, J. Geophys. Res. 79, 2540-2543, 1974.
- Knudsen, W. C. and K. L. Miller, Pioneer Venus Superthermal electron flux measurements in the Venus umbra, J. Geophys. Res. 90, 2695-2702, 1985.
- Krasnopol'sky, V. A., Excitation of oxygen emissions in the night airglow of the terrestrial planets, Planet. Space Sci. 29, 925-929, 1981.

- Krasnopol'sky, V. A., 5577-Å airglow and electron fluxes in the nighttime atmosphere of Venus, *Kosmicheskie Issledovaniya* 20, 742-747, 1982. Translated in *Cosmic Research* 20, 530-534, 1983.
- Opal, C. B., W. K. Peterson and E. C. Beaty, Measurements of secondary-electron spectra produced by electron impact ionization of a number of simple gases, *J. Chem. Phys.* 55, 4100-4106, 1971.
- Rountree, S. P., Electron impact excitation of atomic oxygen: $^3P-3s\ ^5S^0$ and $^3P-3s\ ^3S^0$, *J. Phys. B.* 10, 2719-2725, 1977.
- Rountree, S. P. and R. J. W. Henry, Electron-impact excitation cross sections for atomic oxygen: $^3P-3s\ ^3S^0$, *Phys. Rev. A* 6, 2106-2109, 1972.
- Shyn, T. W., S. Y. Cho and W. E. Sharp, Differential excitation cross-section measurements of $O(^1S)$ by electron impact, *EOS* 66, 989, 1985.
- Stone, E. J. and E. C. Zipf, Electron impact excitation of the $^3S^0$ and $^5S^0$ states of atomic oxygen, *J. Chem. Phys.* 60, 4237, 1974.
- Strickland, D. J. and A. E. S. Green, Electron impact cross sections for CO_2 , *J. Geophys. Res.* 74, 6424, 1969.
- Victor, G. A., P. McKenna and A. Dalgarno, Auroral emission at 1084Å, *Planet. Space Sci.* 24 405, 1976.

Wells, W. C., W. L. Borst and E. C. Zipf, Production of $\text{CO}(a^3\Pi)$ and other metastable fragments by electron impact dissociation of CO_2 , J. Geophys. Res. 77, 69, 1972.

Zipf, E. C. and P. W. Erdman, Electron impact excitation of atomic oxygen: revised cross sections, J. Geophys. Res. 90, 11087-11090, 1985.

Table 1. O(³S) Production Rates.

Predicted O(³S) Production Rates for primary electrons of various energies. The number flux of electrons is normalized to 4 R of 1356Å emission. Three cases are shown:

- A. The Hedin model atmosphere and the Zipf and Erdman (1985) 1356Å Emission cross section.
- B. The Hedin model atmosphere and theoretical excitation cross section for O(⁵S^o) and O(⁵P^e).
- C. The Hedin model atmosphere with the atomic oxygen density doubled and the 1356Å emis-
sion cross section.

<u>Primary energy (eV)</u>	Production Rate (10 ⁶ cm ⁻² s ⁻¹)		
	<u>Case A</u>	<u>Case B</u>	<u>Case C</u>
200	17	9.6	21
300	15	9.4	18
500	12	8.3	16
600	11	7.9	15
800	9.6	7.1	13
1000	8.5	6.5	11

Table 2

Predicted Cameron Band Intensities $\text{CO}(a^3\Pi + X^1\Sigma^+)$ for primary electrons of various energies. The normalization and cases shown are the same as in Table 1.

<u>Primary energy (eV)</u>	<u>Intensity (R)</u>		
	<u>Case A</u>	<u>Case B</u>	<u>Case C</u>
200	84	44	50
300	110	69	61
500	140	96	87
600	150	110	100
800	180	130	120
1000	200	150	130

Table 3

Predicted $O(^1S \rightarrow ^1D)$ Green line Intensities for primary electrons of various energies. The normalization and cases shown are the same as those in Table 1.

<u>Primary Energy (eV)</u>	<u>Intensity (R)</u>		
	<u>Case A</u>	<u>Case B</u>	<u>Case C</u>
200	30	15	26
300	33	21	26
500	39	27	31
600	42	30	33
800	48	35	36
1000	52	40	38

Table 4

Excitations produced by a 100 eV electron depositing its energy in pure atomic oxygen for different values of the fractional ionization, f .

<u>State</u>	<u>Number of Excitations</u>	<u>Fraction of Total Energy (%)</u>
$f = 2 \times 10^{-4}$		
$5S^{\circ}$.0868	.797
$3S^{\circ}$.557	5.32
$1S$.155	0.65
$1D$	2.49	4.93
$f = 2 \times 10^{-5}$		
$5S^{\circ}$.0964	0.885
$3S^{\circ}$	0.579	5.53
$1S$.242	1.02
$1D$	5.14	10.2
$f = 2 \times 10^{-6}$		
$5S^{\circ}$.0982	.902
$3S^{\circ}$.582	5.56
$1S$.264	1.11
$1D$	6.72	13.3

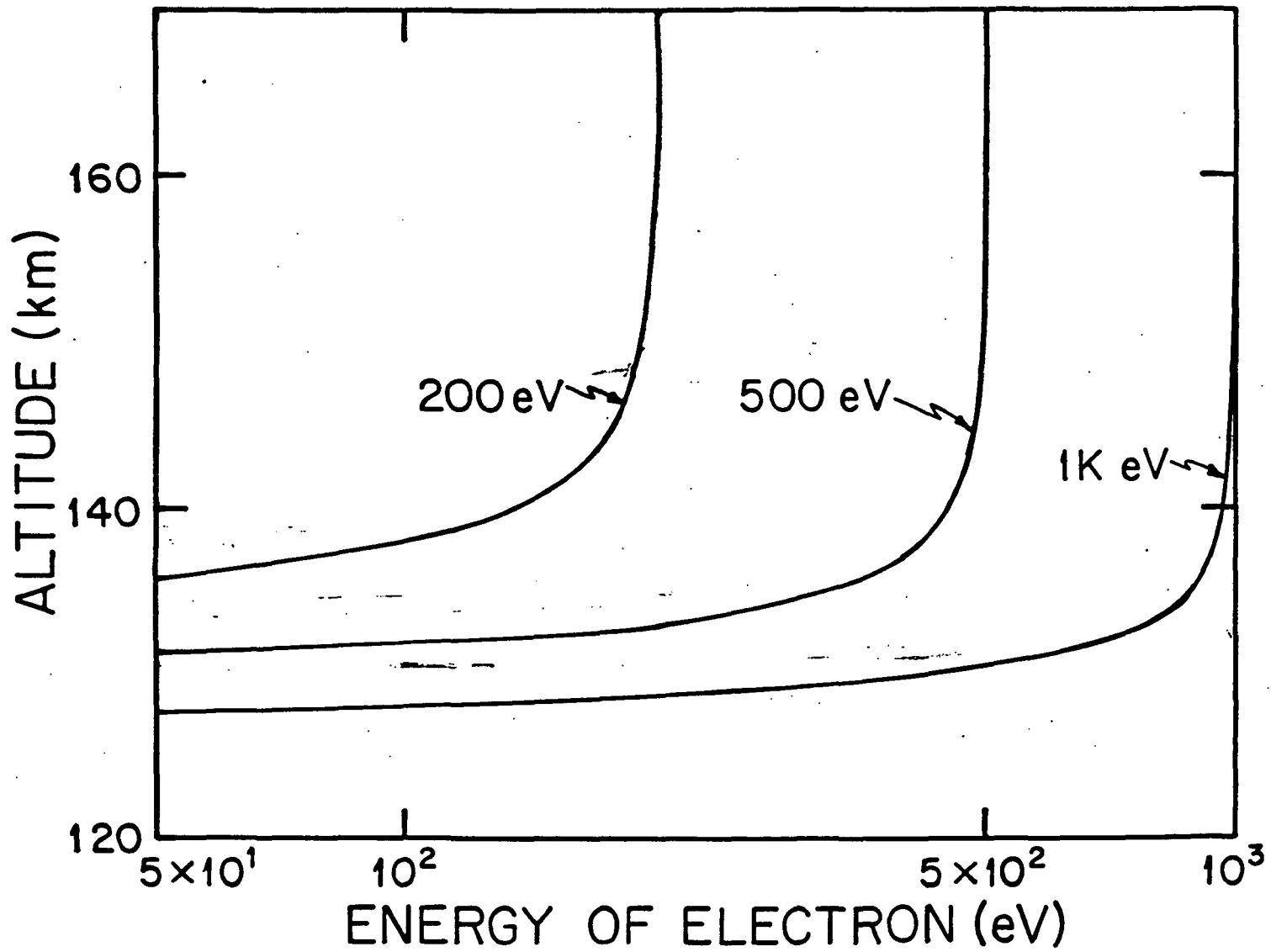


FIGURE 1

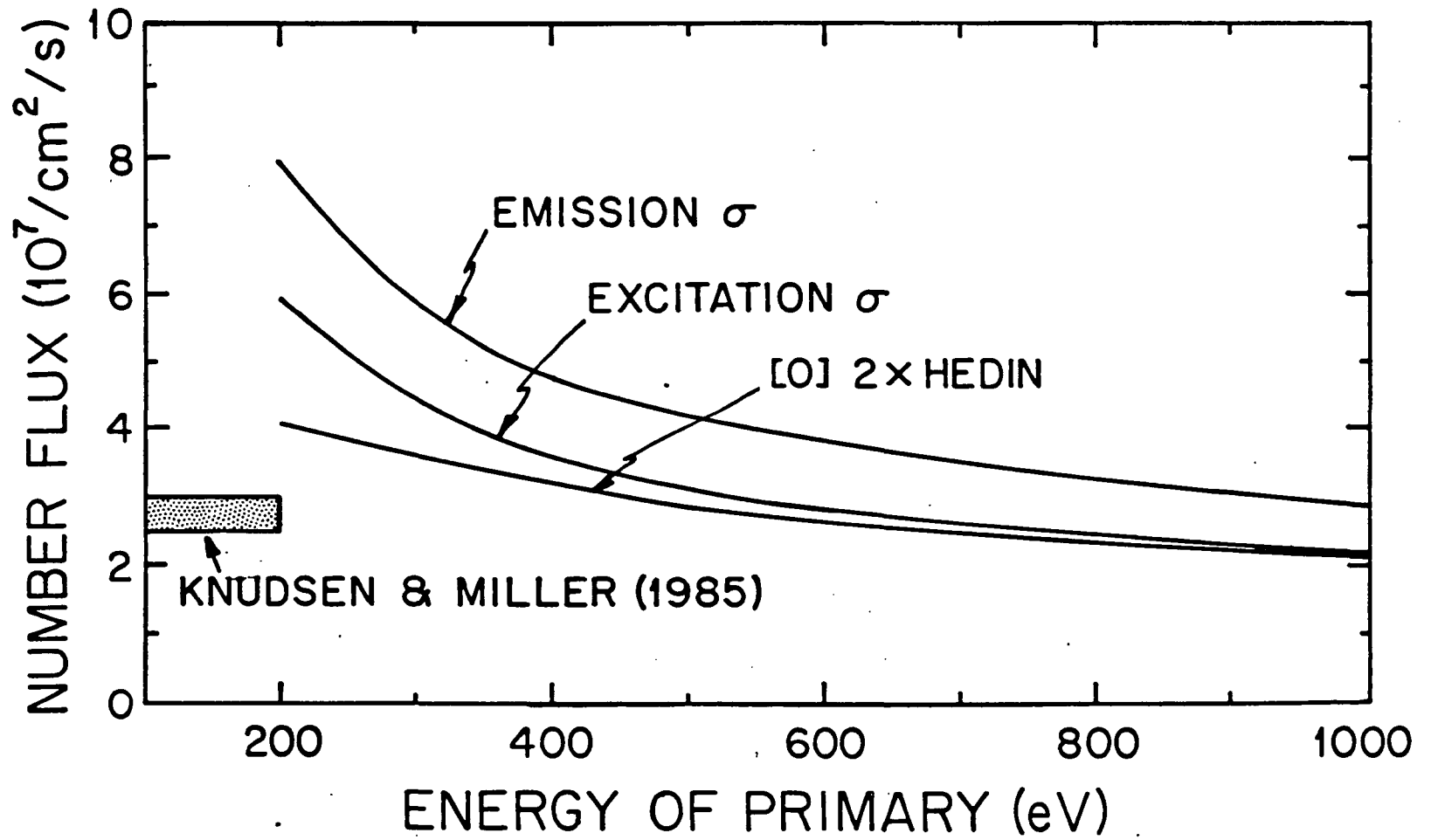


FIGURE 2